Bioorganic & Medicinal Chemistry Letters 23 (2013) 1212–1216

Contents lists available at SciVerse ScienceDirect

Bioorganic & Medicinal Chemistry Letters

journal homepage: www.elsevier.com/locate/bmcl

Optimization of potent and selective dual mTORC1 and mTORC2 inhibitors: The discovery of AZD8055 and AZD2014

Kurt G. Pike [a,*], Karine Malagu [b], Marc G. Hummersone [b], Keith A. Menear [b], Heather M. E. Duggan [b], Sylvie Gomez [b], Niall M. B. Martin [b], Linette Ruston [a], Sarah L. Pass [a], Martin Pass [a]

[a] AstraZeneca, Alderley Park, Macclesfield, Cheshire SK10 4TG, UK
[b] Former employees of KuDOS Pharmaceuticals Ltd., 410 Cambridge Science Park, Milton Road, Cambridge CB4 0WG, UK

ARTICLE INFO

Article history:
Received 13 December 2012
Revised 2 January 2013
Accepted 4 January 2013
Available online 18 January 2013

Keywords:
mTOR
Inhibitor
AZD8055
AZD2014
Kinase

ABSTRACT

The optimization of a potent and highly selective series of dual mTORC1 and mTORC2 inhibitors is described. An initial focus on improving cellular potency whilst maintaining or improving other key parameters, such as aqueous solubility and margins over hERG IC_{50}, led to the discovery of the clinical candidate AZD8055 (**14**). Further optimization, particularly aimed at reducing the rate of metabolism in human hepatocyte incubations, resulted in the discovery of the clinical candidate AZD2014 (**21**).

The mammalian target of rapamycin (mTOR) is a key target in the development of antitumor therapies.[1] Activated by growth factor/mitogenic stimulation activation of the phosphatidylinositol 3-kinase (PI3K)/Akt signaling pathway mTOR is a central regulator of cell growth and proliferation. This PI3K–Akt–mTOR pathway is one of the most frequently dysregulated pathways in cancer.[2] mTOR, a serine/theronine kinase of approximately 289 kDa in size, is a member of the evolutionary conserved eukaryotic PI3K like kinase (PIKK) family of proteins, for example DNA dependent protein kinase (DNA-PK) and Ataxia-telangiectasia mutated (ATM).[3–5]

The known mTOR inhibitor Rapamycin and its analogues (RAD001, CCI-779, AP23573) bind to the FKBP12/rapamycin complex binding domain (FRB), resulting in suppression of signaling to the downstream targets p70S6K and 4E-BP1.[6,7] The potent but non-specific inhibitors of PI3K, LY294002 and wortmannin, have also been shown to inhibit the kinase function of mTOR; however, in this case the catalytic domain of the protein is targeted.[8]

Recently it has been shown that mTOR can exist in an alternative, rapamycin insensitive, complex that signals to Akt.[9] The existence of both a rapamycin sensitive complex (mTORC1) and a rapamycin insensitive complex (mTORC2) may provide an explanation for the differences observed in the earlier work of Brunn et al.[8] and Edinger et al.[10] Rapamycin and its analogues have been shown to activate AKT signaling as a consequence of inhibition of the negative feedback loop downstream of mTORC1.[11] Moreover, this is associated with a shorter time to progression in glioblastoma patients treated with rapamycin suggesting that dual mTORC1 and 2 inhibitors that inhibit AKT signaling could offer greater clinical benefit compared with rapalogues.[12] In addition, dual mTORC1 and mTORC2 inhibitors may exhibit a broader spectrum of clinical activity.

We have previously described the identification of compound **1** from a screening campaign and the subsequent optimization of the scaffold resulting in the discovery of Ku-0063794 (Fig. 1).[13]

Ku-0063794 is a potent inhibitor of mTOR kinase (IC_{50} = 0.0025 μM) and displays a high level of selectivity against other members of the PIKK family (IC_{50} against PI3K isoforms α, β, γ, δ = 8.9, >30, >30 and 5.3 μM, respectively).[14] Ku-0063794 also showed a high level of general kinase selectivity and was inactive against a panel of over 200 kinases when tested at 10 μM. In cells

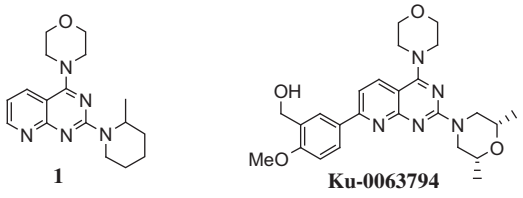

Figure 1. The structures of 1 and Ku-0063794.

* Corresponding author. Address: Mereside, Alderley park, Macclesfield, Cheshire SK10 4TG, UK. Tel.: +44 (0) 1625 512733; fax: +44 (0) 1625 513624.
E-mail address: kurt.pike@astrazeneca.com (K.G. Pike).

0960-894X/$ - see front matter © 2013 Elsevier Ltd. All rights reserved.
http://dx.doi.org/10.1016/j.bmcl.2013.01.019

Table 1
The introduction of basic groups to the C7 aryl substituent

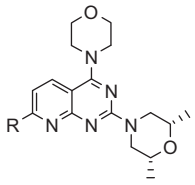

Compd No.	R	pAKT (S^{473}) IC_{50} (μM)	Solubility (μM)	hERG IC_{50} (μM)
Ku-0063794	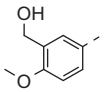	0.24	2.4	8.3
2	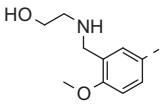	0.062	>1100	27.5
3	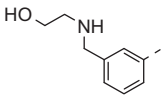	0.137	>2000	13.0
4	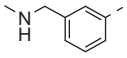	0.303	>1400	17.4
5	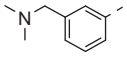	>2.43	—	—

Ku-0063794 has been shown to modulate downstream markers of mTORC1 (inhibition of pS6 at $Ser^{235/236}$ IC_{50} = 0.66 μM) and mTORC2 (inhibition of pAKT at Ser^{473} IC_{50} = 0.24 μM).[15] Ku-0063794 has been shown to be active in mouse xenograft models.[16]

Despite the high affinity of Ku-0063794 for mTOR kinase the moderate cellular potency was felt to offer scope for further improvement. Data generated on Ku-0063794 and close analogues highlighted the similar cellular potencies and structure–activity relationship (SAR) seen with both the pS6 ($S^{235/236}$) and the pAKT (S^{473}) measures. As a result a simplified cascade with the pAKT (S^{473}) cellular measure as the primary assay was introduced. Enzyme data and pS6 ($S^{235/236}$) cellular data was generated on compounds of interest only. In addition, a relatively low aqueous solubility (2.4 μM)[17,18] and relatively high potency against the hERG (human ether-a-go-go-related gene) ion channel (IC_{50} = 8.3 μM)[19] may also present problems for the long term clinical development of Ku-0063794. Consequently, further optimization was initiated to identify highly selective compounds with increased cellular potency, improved aqueous solubility and an improved margin to the hERG IC_{50}.

Our initial strategy to improve aqueous solubility was the introduction of basic functionality, thereby giving a charged molecule at physiological pH. Previous studies had shown that the pendant aryl ring at the C7-position of the Pyridopyrimidine core could tolerate a variety of substituents, although the presence of the benzyl alcohol H-bond donor was known to be advantageous. With this in mind we looked to replace the benzyl alcohol with a range of secondary benzyl amines (Table 1). Such compounds were generally well tolerated with certain examples (e.g., **2**) showing improved potency. As anticipated these compounds showed a dramatic improvement in solubility and a reduction in hERG potency was also observed. Removal of the methoxy group, **3**, did give a slight reduction in potency but excellent solubility was retained. Attempts to introduce tertiary amines in this position resulted in a significant reduction in potency (**5** cf **4**) highlighting the importance of an H-bond donor in that region of the molecule.

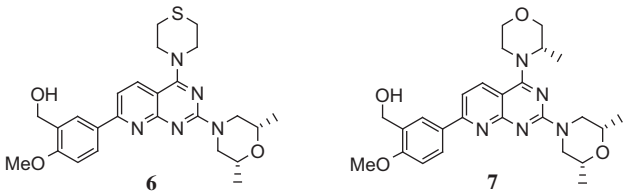

Figure 2. The structures of **6** (pAKT IC_{50} = 2.92 μM) and **7** (pAKT IC_{50} = 0.026 μM).

Despite the improved cellular potency and solubility, **2** showed little oral exposure presumably due to compromised permeability and higher efflux. The apparent permeability (Papp), as measured in MDCKII cells, for Ku-0063794 and **2** in both the A–B and B–A directions are 26/453 nm/s and 150/166 nm/s, respectively.[20,21]

The oxygen of the C4-morpholine has been established as a key pharmacophoric element for this series[13] with attempts to remove this causing a considerable reduction in potency (e.g., **6**). Analogies to other known PIKK family inhibitors would suggest that this oxygen participates in a key interaction with the hinge region of the kinase. However, conservative changes in this region are tolerated, and in particular the 3*S*-methyl morpholine containing compound, **7**, was identified as having significantly improved cellular potency (Fig. 2). Interestingly, a modest increase in solubility was also observed for this compound (16 μM).

The impact of replacing the C4-morhpoline with a 3*S*-methyl morpholine has been examined across a range of analogues. An analysis of matched pairs (Fig. 3) shows a consistent improvement in cellular potency with an average increase of 0.73 ± 0.11 in pIC_{50}. A similar analysis also highlights a trend for improved solubility, on average between 5- and 10-fold; however, no assessment of the solid state properties of these compounds has been made. These observations are consistent with the 3*S*-methyl group either locking the morpholine ring in a more favorable conformation for binding or accessing a small lipophilic pocket upon binding. The increase in solubility may reflect a lowering in crystal lattice energy due to disrupted crystal packing upon the addition of the methyl group. Similar SAR regarding the hinge binding morpholine has recently been described for other PIKK inhibitors although the observations are subtly different between series.[22]

Aqueous solubility is often negatively correlated with lipophilicity, hence another strategy adopted was to reduce the lipophilic-

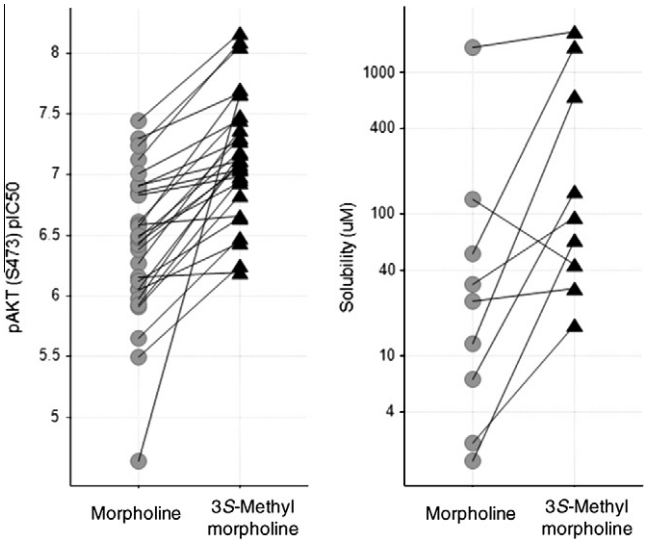

Figure 3. Matched pairs plot highlighting the impact of switching from a morpholine to a 3*S*-methyl morpholine on both cellular pIC_{50} and solubility.

Table 2
Impact of switching from a Pyridopyrimidine to a Pteridine core

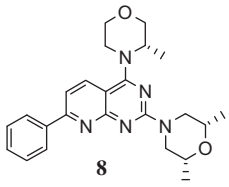

8

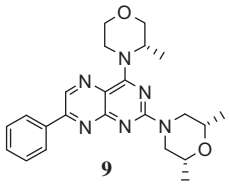

9

Compd No.	pAKT (S^{473}) IC_{50} (μM)	C log *P*	log *D*	Solubility (μM)	hERG IC_{50} (μM)
8	0.094	4.14	3.75	66	4.0
9	0.103	3.40	>4.0	13	13.2

ity of the core. Pteridine analogues (e.g., **9**) were tolerated; however, the anticipated reduction in lipophilicity (based on C log *P* prediction)[23] was not reflected in the measured log *D* values[18] and indeed a reduction in solubility was observed (Table 2).

We next focused our attention on the C2 substituent. A wide range of amines were tolerated including non-morpholine substituents, basic amines and acyclic amines (**8**–**12**) as were aromatic substituents, such as compound **13**; however, when assessing the overall balance of properties the 3*S*-methyl morpholine analogue, **14**, appeared optimal (Table 3).

Compound **14** is a potent inhibitor of mTOR kinase (IC_{50} = 0.00013 μM) and displays a high level of selectivity against other members of the PIKK family (IC_{50} against PI3K isoforms α, β, γ, δ = 3.6, 19, 3.2 and 15 μM, respectively) and was inactive against a general panel of over 200 kinases when tested at 10 μM. Unlike rapamycin, **14** inhibits both mTORC1 and mTORC2 in cells with similar potencies (pS6 ($S^{235/236}$) IC_{50} = 0.027 μM, pAKT (S^{473}) IC_{50} = 0.024 μM). Compound **14** also demonstrates a more complete inhibition of phosphorylation of mTORC1 substrate 4E-BP1 ($Thr^{37/46}$) compared to rapamycin in MCF-7 cells and was also shown to inhibit pAKT (S^{473}) in this cell line whereas rapamycin treatment resulted in an activation of AKT as a consequence of inhibition of a negative feedback loop.[24] Compound **14** has been shown to modulate substrates of both mTORC1 and 2 in vivo and

Table 3
Modifications to the C2 amine

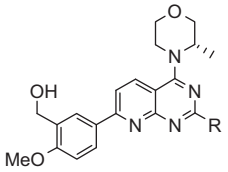

Compd No.	R	pAKT (S^{473}) IC_{50} (μM)	Solubility (μM)	hERG IC_{50} (μM)
8		0.094	66	4.0
10		0.060	13	8.0
11		0.166	>1200	>32
12		0.061	170	17.0
13		0.141	26	>32
14		0.024	30	30.4

Table 4
Modifications to the C7 benzyl amine functionality

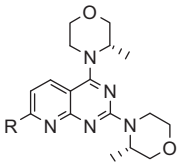

Compd No.	R	pAKT (S^{473}) IC_{50} (μM)	Solubility (μM)	hERG IC_{50} (μM)	Hu Heps (μL/min/10^6 cells)
15	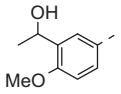	0.090	160	>32	37.8
16	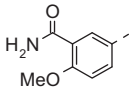	0.017	>690	>32	33.2
17	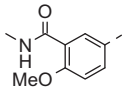	0.009	44	>32	14.3
18	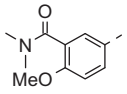	2.83	>640	>32	4.3

Table 5
Modifications to the C7 methoxy and amide substituents

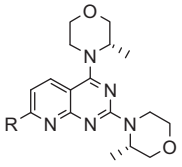

Compd No.	R	pAKT (S^{473}) IC_{50} (μM)	Solubility (μM)	hERG IC_{50} (μM)	Hu Heps (μL/min/10^6 cells)
19	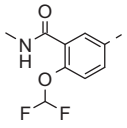	0.026	190	24.2	14.9
20	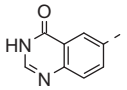	0.358	110	>32	176.4
21	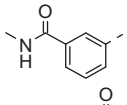	0.080	>600	47.5	<4.2
22	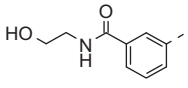	0.041	>870	>32	<5.4

delivers a dose-dependent tumor growth inhibition in mouse xenograft models.[24] Compound **14** was subsequently selected for clinical development and referred to as AZD8055.

Despite its promising profile in preclinical disease models, AZD8055 was found to exhibit high turnover in human hepatocytes (36.4 μL/min/10^6 cells) and also showed lower bioavailability in rat compared with mouse (12% cf 81%). The high turnover of AZD8055 in human hepatocytes, combined with inconsistent rodent pharmacokinetics (PK), was felt to constitute a considerable

risk when trying to predict clinical exposure and hence optimization was continued to identify compounds with an increased confidence of achieving the required clinical exposure.

The metabolism of functional groups such as benzyl alcohols and aryl–methyl ethers is well precedented and were postulated as potential metabolic liabilities in AZD8055. Steric crowding of the benzyl alcohol, such as in compound **15**, had little impact on human hepatocyte metabolism (Table 4). A primary amide could be used to replace the benzyl alcohol generating a potent compound with a dramatically increased aqueous solubility (**16**), although the rate of human hepatic turnover remained high. Substitution on the amide, **17**, did reduce the rate of turnover in human hepatocytes and generally maintained the excellent properties of the molecule, albeit with a reduction in aqueous solubility. A further reduction in hepatic turnover was observed for the tertiary amide **18**; however, this change was associated with a significant reduction in potency again highlighting the importance of an H-bond donor in this vicinity. Limited attempts were made to replace the C7 phenyl ring with aromatic heterocycles but such compounds lost activity (data not shown).

Strategies to reduce potential metabolism of the methoxy group, such as difluorination (**19**) or cyclisation (**20**), were broadly tolerated but failed to deliver a reduction in hepatic turnover (Table 5). Removal of the methoxy group (**21**), however, did result in a compound with good cellular potency and low hepatic turnover. Compound **21** showed excellent aqueous solubility, margin to the hERG IC_{50} and was shown to have good oral exposure in both rat and mouse. Variation of the amide substituent did result in modest improvements in potency with compound **22**, in particular, showing an attractive in vitro profile. However, **22** failed to deliver oral exposure in rodents.

Compound **21** is a potent inhibitor of mTOR kinase (IC_{50} = 0.0028 μM) and displays a high level of selectivity against other members of the PIKK family (IC_{50} against PI3K isoforms α, β, γ, δ = 3.8, >30, >30 and >29 μM, respectively) and was inactive against a general panel of over 200 kinases when tested at 10 μM. Compound **21** inhibits both mTORC1 and mTORC2 in vitro (pS6 ($S^{235/236}$) IC_{50} = 0.2 μM, pAKT (S^{473}) IC_{50} = 0.08 μM) and has shown dose-dependent tumor growth inhibition in a mouse MCF7 xenograft model alongside modulation of mTORC1 and mTORC2 biomarkers.[25] Compound **21** shows consistent exposure in rodents and a low turnover in human hepatocyte incubations and was subsequently selected for clinical development and referred to as AZD2014. A comparison of key in vitro parameters, including potency, solubility, protein binding[26] and rodent PK,[27] for Ku-0063794, AZD8055 and AZD2014 is given in Table 6.

The general synthesis of compounds **2**–**5** is shown in Scheme 1.[28] Reaction of 2,6-dichloronicotinic acid (**23**) with liquid ammonia at elevated temperature and pressure results in the selective introduction of an amino group into the C2 position and subsequent conversion of the carboxylic acid to the primary amide, via the acyl chloride intermediate, generates **24** which can then be cyclised with oxalyl chloride to complete the Pyridopyrimidine scaffold (**25**). Chlorination with phosphorous oxychloride results in the trichloro intermediate **26** and selective installation of the C4 amine is achieved by reaction with the desired amine at low temperature (**27**). Reaction with a second amine at elevated temperature is then used to install the C2 amine functionality (**28**). Finally, the C7 aryl substituent can be installed using palladium mediated cross couplings with desired boronic ester to give Ku-0067394. Conversion of the benzyl alcohol to a benzyl chloride and subsequent displacement with the desired amine generates compounds **2**–**5**.

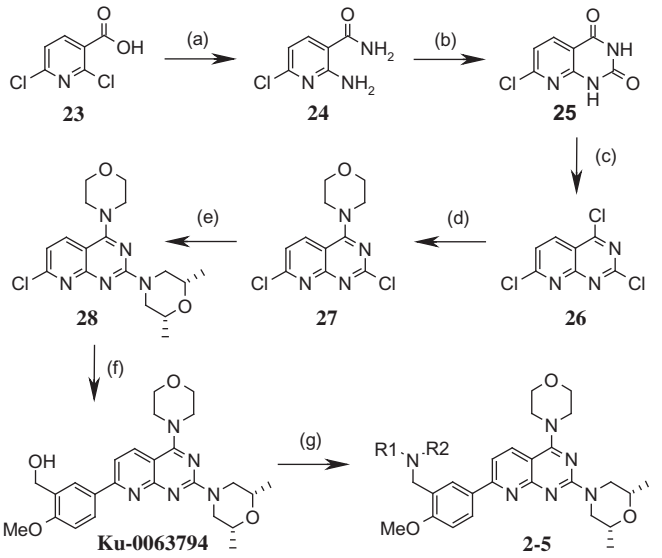

Scheme 1. Reagents and conditions: (a) (i) NH_3(liq), 18 bar, 130 °C, 90%; (ii) $SOCl_2$, THF, rt; (iii) NH_3(g), THF, rt, 92% over 2 steps; (b) $(COCl)_2$, toluene, 115 °C, 95%; (c) $POCl_3$, Hünigs base, toluene, 100 °C, 48%; (d) morpholine, Hünigs base, CH_2Cl_2, 0 °C–rt, 92%; (e) 2,6-dimethylmorpholine, Hünigs base, DMA, 70 °C, 45%; (f) [2-methoxy-5-(4,4,5,5-tetramethyl-1,3,2-dioxaborolan-2-yl)phenyl]methanol, $Pd(PPh_3)_4$, Na_2CO_3, toluene/ethanol, 140 °C, 75%; (g) (i) MsCl, Et_3N, CH_2Cl_2, rt, 99%; (ii) selected amine, K_2CO_3, Et_3N, DMF, 40 °C.

The general synthesis of compounds **14**–**22** is shown in Scheme 2.[29] 3*S*-Methylmorpholine is installed sequentially at the C4 then C2 positions of trichloro intermediate **26** to generate **29** which can then be reacted with a range of boronic esters using palladium mediated cross couplings to generate compounds **14**–**22**. Analogous procedures were used to deliver compounds **6**–**8** and compounds **10**–**13**. Pteridine compound **9** was synthesized from the commercially 7-phenylpteridine-2,4-diol using chemistry analogous to that described in Scheme 1.

Table 6
Comparison of key pre-clinical parameters

	Ku-0063794	AZD8055	AZD2014
mTOR IC_{50} (μM)	0.0025	0.00013	0.0028
pAKT (S^{473}) IC_{50} (μM)	0.24	0.024	0.080
pS6 ($S^{235/236}$) IC_{50} (μM)	0.66	0.027	0.2
log *D*	3.25	3.23	3.16
Solubility (μM)	2.4	30	>600
f_u (Mouse)	0.01	0.04	0.05
f_u (Rat)	0.15	0.08	0.09
f_u (Human)	0.08	0.13	0.05
Hu Heps (μL/min/10^6 cells)	—	36.4	<4.2
Mouse clearance (mL/min/kg)	3.1	42.8	10.4
Mouse bioavailability	61%	81%	>100%
Rat clearance (mL/min/kg)	35.8	36.6	12.6
Rat bioavailability	33%	12%	40%
hERG IC_{50} (μM)	8.3	30.4	47.5

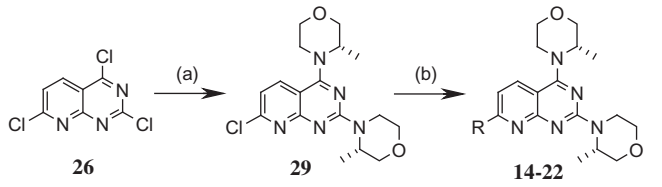

Scheme 2. Reagents and conditions: (a) (i) 3*S*-Methylmorpholine, Hünigs base, CH_2Cl_2, 0 °C–rt, 87%; (ii) 3*S*-methylmorpholine, Hünigs base, DMA, 70 °C, 71%; (b) selected boronic ester, $Pd(PPh_3)_4$, Na_2CO_3, toluene/ethanol, 140 °C or selected boronic ester, $Pd(PPh_3)_4$, K_2CO_3, MeCN/water, 150 °C.

In summary, we have shown how iterative SAR investigations have been used to optimize the cellular potency, aqueous solubility and hERG potency of lead compound Ku-0063794 to deliver the clinical candidate AZD8055. Further optimization focused on reducing turnover in human hepatocytes and resulted in the identification of the clinical candidate AZD2014, which was believed to offer a reduced human PK risk compared to AZD8055. AZD8055 and AZD2014 are potent and selective dual mTORC1 and mTORC2 inhibitors which show a differentiation from rapamycin in vitro and have demonstrated dose-dependent tumor growth inhibition in mouse xenograft models. AZD8055 was evaluated in a phase I clinical study in patients with advanced tumors but is no longer in clinical development. AZD2014 is currently in phase I.

Acknowledgments

The authors would like to thank Christine Chresta and Tom Harding for their help in preparing the biological data presented and Dr. Kin Tam for his help preparing the physicochemical data presented.

References and notes

1. Huang, S.; Houghton, P. J. *Curr. Opin. Pharmacol.* **2003**, *3*, 371.
2. Yap, T. A.; Garrett, M. D.; Walton, M. I.; Raynaud, F.; de Bono, J. S.; Workman, P. *Curr. Opin. Pharmacol.* **2008**, *8*, 393.
3. Brown, E. J.; Albers, M. W.; Shin, T. B.; Ichikawa, K.; Keith, C. T.; Lane, W. S.; Schreiber, S. L. *Nature* **1994**, *369*, 756.
4. Sabatini, D. M.; Erdjument-Bromage, H.; Lui, M.; Tempst, P.; Snyder, S. H. *Cell* **1994**, *78*, 35.
5. Abraham, R. T. *Curr. Opin. Immunol.* **1996**, *8*, 412.
6. Fingar, D. C.; Salama, S.; Tsou, C.; Harlow, E.; Blenis, J. *Genes Dev.* **2002**, *16*, 1472.
7. Fingar, D. C.; Richardson, C. J.; Tee, A. R.; Cheatham, L.; Tsou, C.; Blenis, J. *Mol. Cell. Biol.* **2004**, *24*, 200.
8. Brunn, G. J.; Williams, J.; Sabers, C.; Wiederrecht, G.; Lawrence, J. C., Jr.; Abraham, R. T. *EMBO J.* **1996**, *15*, 5256.
9. Sarbassov, D. D.; Ali, S. M.; Sabatini, D. M. *Curr. Opin. Cell Biol.* **2005**, *17*, 596.
10. Edinger, A. L.; Linardic, C. M.; Chiang, G. G.; Thompson, C. B.; Abraham, R. T. *Cancer Res.* **2003**, *63*, 8451.
11. Sun, S. Y.; Rosenberg, L. M.; Wang, X.; Fu, H.; Khuri, F. R. *Cancer Res.* **2005**, *65*, 7052.
12. Cloughesy, T. F.; Yoshimoto, K.; Nghiemphu, P.; Brown, K.; Dang, J.; Zhu, S.; Hsueh, T.; Chen, Y.; Wang, W.; Youngkin, D.; Liau, L.; Martin, N.; Becker, D.; Bergsneider, M.; Lai, A.; Green, R.; Oglesby, T.; Koleto, M.; Trent, J.; Horvath, S.; Mischel, P. S.; Mellinghoff, I. K.; Sawyers, C. L. *PLoS Med.* **2008**, *5*, e8.
13. Malagu, K.; Duggan, H.; Menear, K.; Hummersone, M.; Gomez, S.; Bailey, C.; Edwards, P.; Drzewiecki, J.; Leroux, F.; Jimenez Quesada, M.; Hermann, G.; Maine, S.; Molyneaux, C.; Le Gall, A.; Pullen, J.; Hickson, I.; Smith, L.; Maguire, S.; Martin, N.; Smith, G.; Pass, M. *Bioorg. Med. Chem. Lett.* **2009**, *19*, 5950.
14. Inhibition of mTOR kinase was evaluated in a high-throughput assay using α screen capture complex technology (Perkin-Elmer) with a recombinant truncated FLAG-tagged mTOR (amino acids 1362–2549, expressed in HEK293 cells). The activity of the lipid kinases, class I PI3Ks α, β, γ, δ was measured with the lipid PIP2 as substrate. More detailed description of the assay conditions are described in Ref. [24]
15. MDA-MB-468 cells were exposed for 2 h to increasing concentrations of compound. At the end of the incubation period cells were fixed, washed and probed with antibodies against S^{473} pAKT or against $S^{235/236}$ phosphorylated S6 (pS6). Levels of phosphorylation were assessed using an Acumen laser scanning cytometer (TTP Labtech). Figures quoted are the mean of at least 3 determinations and the standard error in the mean (pIC_{50}) was <0.3.
16. Pike, K. G.; Menear, K.; Gomez, S.; Malagu, K.; Hummersone, M.; Pass, M.; Duggan, H.; Hickson, I.; Chresta, C.; Davies, B.; Martin, N.; Smith, G. Presented at the 241st National Meeting of the American Chemical Society: Anaheim, CA, March 2011; Abstract MEDI#188.
17. Assessments of aqueous solubility were made after an incubation of 24 h in pH 7.4 phosphate buffer. After centrifugation, analysis of the supernatant liquid was performed by LC–UV to quantify the amount of compound in solution. Further details are contained in Ref. [17].
18. Buttar, D.; Colclough, N.; Gerhardt, S.; MacFaul, P. A.; Phillips, S. D.; Plowright, A.; Whittamore, P.; Tam, K.; Maskos, K.; Steinbacher, S.; Steuber, H. *Bioorg. Med. Chem.* **2010**, *18*, 7486.
19. Redfern, W. S.; Carlsson, L.; Davis, A. S.; Lynch, W. G.; MacKenzie, I.; Palethorpe, S.; Siegl, P. K. S.; Strang, I.; Sullivan, A. T.; Wallis, R.; Camm, A. J.; Hammond, T. G. *Cardiovasc. Res.* **2003**, *58*, 32; Waring, M. J.; Johnstone, C.; McKerrecher, D.; Pike, K. G.; Robb, G. *Med. Chem. Commun.* **2011**, *2*, 775.
20. Monolayers of MDCKII (Madin Darby Canine Kidney Cells) cells transfected with the human MDR1 (Multi-Drug Resistance 1) transporter protein were cultured in transwells and used to study the permeability and efflux potential of compounds at a concentration of 10 μM.
21. Keogh, J. P.; Kunta, J. R. *Eur. J. Pharm. Sci.* **2006**, *27*, 543.
22. Zask, A.; Kaplan, J.; Verheijen, J. C.; Richard, D. J.; Curran, K.; Brooijmans, N.; Bennett, E. M.; Toral-Barza, L.; Hollander, I.; Ayral-Kaloustian, S.; Yu, K. *J. Med. Chem.* **2009**, *52*, 7942.
23. *C*log*P* values were calculated using the commercially available package *C*log*P* v4.3 from BioByte Corp., 201 W. 4th Str., #204 Claremont, CA 91711-4707.
24. Chresta, C. M.; Davies, B. R.; Hickson, I.; Harding, T.; Cosulich, S.; Critchlow, S. E.; Vincent, J. P.; Ellston, R.; Jones, D.; Sini, P.; James, D.; Howard, Z.; Dudley, P.; Hughes, G.; Smith, L.; Maguire, S.; Hummersone, M.; Malagu, K.; Menear, K.; Jenkins, R.; Jacobsen, M.; Smith, G. C. M.; Guichard, S.; Pass, M. *Cancer Res.* **2010**, *70*, 288.
25. Guichard, S. M.; Howard, Z.; Heathcote, D.; Roth, M.; Hughes, G.; Curwen, J.; Yates, J.; Logie, A.; Holt, S.; Chresta, C. M.; Davies, B. R.; Malagu, K.; Hummersone, M.; Pass, S. L.; Green, S.; Pass, M. Presented at AACR Annual Meeting: Chicago, 2012; Abstract 917. Further details of the in vitro and in vivo profile of AZD2014 (**21**) will be presented in future publications.
26. The plasma protein binding of compounds was measured using equilibrium dialysis technique and is quoted as the Fraction unbound (f_u). Values for AZD8055 and AZD2014 were generated in undiluted plasma at a range of drug concentrations using radiolabelled material ([^{3}H]-AZD8055 or [^{14}C]-AZD2014); no concentration dependency was observed. A more detailed description of the equilibrium dialysis assay conditions are described in Chiou, W. L.; Robbiel, G.; Chung, S. M.; Wul, T.-C.; Mal, C. *Pharm. Res.* **1998**, *15*, 1474.
27. Mouse clearance values were obtained following an IV dose of 10 μmol/kg to CD-1 out bred mice and rat clearance values were obtained following an IV dose of either 1 μmol/kg (Ku-0063794) or 4 μmol/kg (AZD8055 and AZD2014) to CR-Han Wistar rats. The compounds were dosed as a solution. Bioavailability values were calculated following an oral dose of 20 μmol/kg in mouse and either 6 μmol/kg (Ku-0063794) or 20 μmol/kg (AZD8055 and AZD2014) in rat.
28. Hummersone, M. G.; Gomez, S.; Menear, K. A.; Smith, G. C. M.; Malagu, K.; Duggan, H. M. E.; Cockcroft, X.-L. F.; Hermann, G. J. WO2007060404, 2007.
29. Duggan, H. M. E.; Leroux, F. G. M.; Malagu, K.; Martin, N. M. B.; Menear, K. A.; Smith, G. C. M. WO2008023161, 2008.